SDC-91-138

SDC
SOLENOIDAL DETECTOR NOTES

SOME PHYSICS REQUIREMENTS FOR TRIGGERING IN THE INTERMEDIATE TRACKING SYSTEM OF SDC

November 22, 1991

Hans-Jochen Trost
Argonne National Laboratory

The submitted manuscript has been authored by a contractor of the U. S. Government under contract No. W-31-109-ENG-38. Accordingly, the U. S. Government retains a nonexclusive, royalty-free license to publish or reproduce the published form of this contribution, or allow others to do so, for U. S. Government purposes.

ANL/HEP/TR-91/100
SDC-91-00138

Some physics requirements for triggering in the intermediate tracking system of SDC*

HANS-JOCHEN TROST

High Energy Physics Division - 362 -
Argonne National Laboratory
9700 S. Cass Ave., Argonne, IL 60439-4815, USA

22 November 1991

ABSTRACT

I have investigated trigger requirements for the intermediate tracking system of the SDC detector, using muons in the final states of some physics processes of interest and relevance to the program envisaged to be pursued at the SSC. The study is done at the physics event generator level with the PYTHIA package, augmented by a very simplistic simulation of the momentum measurement expected from the intermediate tracking system. For the range in pseudorapidity of $|\eta| = 1.7 - 2.5$, I find a subdivison into four bins sufficient to ensure that the width of the transverse momentum trigger threshold will not be dominated by the lack of knowledge of the polar angle. In addition, the azimuthal resolution has to be better than 1 *mrad* to allow transverse momentum thresholds from $p_t \approx 10\ GeV/c$ up to and beyond $p_t = 20\ GeV/c$ to be implemented which are needed to accomplish the physics goals.

* Work supported by the U.S. Department of Energy, Division of High Energy Physics, Contract W-31-109-ENG-38

1. Introduction

The region of pseudorapidity beyond the reasonable reach of a central tracking system of the SDC detector, $|\eta| \geq 1.4 - 1.8$, constitutes an important part of the acceptance for the measurement of physics processes of interest at the SSC.[1-3] Technically, this region presents a strong challenge for constructing a detector able to survive there and measure charged particles with sufficient quality.[1,4,5]

In the present note, I investigate some requirements for track triggering in the intermediate angle region using a few processes of interest within the standard model of strong and electroweak interactions which naturally take a front row seat among the candidate processes for being studied at the SSC. I restrict myself to muon signatures of final states and the required characteristics of a tracking system to trigger on these muons. The philosophy assumed here[6] for the trigger emphasizes accepting as many "good" tracks as possible over getting rid of fakes and other noise. While, for historical reasons, only muons are used and mentioned, the results apply more or less for electrons as well. In the practical applications of a real experiment, different background contributions will arise for muons and electrons, like production in decays for the former and photon conversion for the latter. These contributions are completely ignored in the present work; they would raise the trigger rates but would otherwise not affect the discussion below.

2. Methods and tools

I have used the PYTHIA event generator version 5.4[7] for a number of processes: hard QCD scattering, production of $b\bar{b}$, $t\bar{t}$ ($m_t = 150\ GeV/c^2$), inclusive Z^0, $Z^0 + jet$, nonresonant Z^0 pairs and the neutral Higgs boson, H^0 (for $m_H = 140\ GeV/c^2$ and $m_H = 400\ GeV/c^2$). For the Higgs boson, I have also looked specifically at the subprocess $H^0 \rightarrow Z^0 Z^0 \rightarrow \mu^+\mu^-\mu^+\mu^-$ which due to its small cross section and outstanding signature has received a lot of attention

already in the past. (For the light mass which is less than twice the mass of the Z^0 boson, one of the two decay bosons is to be taken virtual, to account for the proper kinematics. PYTHIA takes care of that properly, and this is implicitly to be understood whenever this channel is referred to below.) I have used a cut on the minimal transverse momentum appearing in the hard scattering processes defining these final states of $q_{t,min} = 1\ GeV/c$ except for the case $Z^0 + jet$ which denotes a subset of the inclusive Z^0 production and is analysed only for $q_{t,min} = 25\ GeV/c$.†

For the purpose of the trigger study, I assume a configuration of three tracking stations, placed at distances of 3.1 m, 3.5 m and 3.9 m from the nominal interaction point. Each of these stations is supposed to deliver a point measurement (z_i, φ_i), $i = 1, 2, 3$, in a given range of pseudorapidity η (and thereby polar angle θ). The practical requirement for a track to be recognizable is to have a point from each of the three stations. The change of the observed azimuthal angle φ across the three stations can be determined from the points in the first and third stations. To obtain these numbers from the generated event for a given particle (*i.e.* muon in the present study), I pick up the transverse momentum p_t, the polar angle θ and the pseudorapidity $\eta = -ln(tan(\theta/2))$. For the change $p_{t,kick}$ of the transverse momentum and the change φ_{kick} of the azimuthal angle relative to the values at the interaction point, I use the relations

$$\begin{aligned} p_{t,kick} &\approx 0.3\ GeV/c \cdot (Tm)^{-1} \cdot \int B dl(\eta) \\ p_t &= \frac{p_{t,kick}}{sin\varphi_{kick}} \end{aligned} \tag{1}$$

with the field integrals taken from a simple analytical approximation to the curves shown in Fig.9 of the SDC Letter of Intent[2] (Fig.1). As a simplification, I assume

† With this choice, the cross section for this final state will be overestimated somewhat as the cross section calculation diverges at small q_t,[8] the divergence being compensated by the non-QCD-radiative and other parts of the total Z^0 production cross section. As I am interested in this process as a background source in the present context, this is not misleading in a harmful way.

that at any angle a homogeneous axial field is seen by the charged particles with a total field integral given by the beforementioned curve. Beyond the third station I take the field to drop to zero immediately. Under these assumptions, all charged particle trajectories have circular projections in the (x, y) plane transverse to the beam axis. The transverse radii r_i and azimuthal angles φ_i measured by the three stations follow from

$$\begin{aligned} r_i &= z_i \, tan\theta_i \\ R &= \frac{r_3}{2sin(\varphi_{kick}/2)} \\ sin\varphi_i &= \frac{r_i}{2R} \end{aligned} \tag{2}$$

where R gives the radius of curvature of the particle, and $\varphi_3 \equiv \varphi_{kick}/2$ is just a relabeling of one quantity. In the actual experiment, the transverse momentum can then be calculated from the formula

$$tan\frac{\varphi_{kick}}{2} = \frac{r_3 sin\varphi_3 - r_1 sin\varphi_1}{r_3 cos\varphi_3 - r_1 cos\varphi_1} \tag{3}$$

which implies as a constraint the assumption that the track originates from the interaction point, $(x, y) = (0, 0)$. Reconstructing the transverse momentum of a charged particle thus hinges on the ability to measure the angles φ_1 and φ_3 and the radii r_1 and r_3. As it does not matter where the angle $\varphi = 0$ is located, I will look at this problem in terms of the difference $\Delta\varphi = |\varphi_3 - \varphi_1|$ (also ignoring the charge sign). For the radial coordinate, I will assume that the tracking system is read out in four bins of pseudorapidity of width $\Delta\eta = 0.2$ covering the range $|\eta| = 1.7 - 2.5$. To fix a single unique radius for each bin, I use the average of the polar angles of the bin edges.

I have generated 400000 events for the QCD case, 30000 events each for the $b\bar{b}$ and $t\bar{t}$ cases, 10000 events each for the $4\mu^{\pm}$ final states, and 40000 events each in all remaining cases. The events are analyzed and distributions accumulated "on

the fly" with no program change occurring for any of the processes. Whenever data samples are compared on a common scale, I have set this scale to one year of SSC design luminosity, *i.e.* $10^7\ s \cdot 10^{33}\ cm^{-2}s^{-1} = 10\ fb^{-1}$. A useful, easy-to-remember relation in this context is that the integrated luminosity in units of nb^{-1} needed for a certain number of events is equal to the time in seconds it takes to produce and measure those events.

3. Analysis and results

For the following, I take the production of the neutral Higgs boson as the signal process of interest, and all other processes as possible backgrounds. I begin with looking at the overall spatial distribution of muons, *i.e.* for the present purpose the distribution over rapidity y (Fig.2). The mundane processes like hard QCD scattering and Z^0 production show fairly flat distributions while the muons from the $t\bar{t}$ and neutral Higgs boson final states appear more centrally, due to the high mass of the intermediate states (the top quark and antiquark and the Higgs boson respectively) involved. The large differences in the rates for muons are dictated by corresponding large differences in the production cross sections. In the cascades $H^0 \rightarrow Z^0 Z^0 \rightarrow 4\mu^{\pm}$, the branching ratios in the two steps create another large rate penalty. No restrictions on momenta or decay channels, except for the cascades just mentioned, have been imposed; even for the four-muon final state, all other muons that may have been produced alongside with the Higgs boson, *e.g.* from beam fragmentation and hadronization, are included as well.

The transverse momentum distributions for the same event samples (Fig.3) show even more outstanding differences in their shapes: The QCD processes overall have their spectra rapidly decaying with increasing transverse momentum while the processes involving high masses produce distributions extending out to quite high transverse momenta. In fact, requiring a minimum transverse momentum beyond a few GeV/c, to beyond about 10 GeV/c, will cut the uninteresting QCD processes already by large factors while about half of the $t\bar{t}$

production and most of the Higgs boson production will be kept. A closer look at the transverse momentum distributions in four bins of pseudorapidity covering the intermediate angle region ($|\eta| = 1.7 - 2.5$) shows that this observation remains valid even locally (Fig.4).

A further handle on reducing the undesired processes when looking for the all-charged-lepton decays of the neutral Higgs boson is the multiplicity of charged leptons (Fig.5). The hard requirement of having to detect all four decay leptons to reconstruct the Higgs boson has already some strong implications for the geometrical acceptance to be provided.[9-13] Depending on the mass of the Higgs boson, the geometrical acceptance for the complete four-lepton final state of a detector covering the pseudorapidity out to $|\eta| = 2.5$ is in the range of $40 - 75\%$. The study of Michael Barnett, Kevin Einsweiler and Ian Hinchliffe[13] prepared for the SDC Letter of Intent[2] presents some details on the correlations induced and combined effects of requiring a number of leptons above some threshold of transverse momentum and within some range of pseudorapidity (Figs.8 and 14 of ref.13). A trigger threshold of 20 GeV/c for the transverse momentum turns out to be a viable compromise between the overall rate such a trigger has[2] and the acceptance of it (see Fig.3 and ref.13). Thus, a representative basic configuration for triggering is to require leptons to appear with $p_t \geq 20\ GeV/c$ and $|\eta| \leq 2.5$. These cuts strongly reduce the acceptance for all background processes in particular when demanding high muon multiplicities (Fig.6). By looking at the acceptances for multiple muons as a function of the range of pseudorapidity covered, the differences in the kinematic configurations become evident that I had mentioned earlier (Fig.7, cf. also Fig.2): The background processes show their muons concentrated more towards the beam axis while the top and Higgs final states populate the region transverse to the axis much more. Figure 7 also shows that, in the cases where muonic gauge boson decays ($W \rightarrow \mu\nu_\mu$ and/or $Z^0 \rightarrow \mu^+\mu^-$) are supposed to supply the or a tag for the process under consideration, muons from the "underlying" event can have a significant impact on possibly satisfying any given trigger setting. These acceptances combined

with the corresponding cross sections (Table 1) give the basic trigger efficiencies for a perfect detector. The table shows that without the kinematic cuts even a requirement for four muons (if that could be experimentally realized) would saturate the expected data acquisition capacity of 100 Hz easily while after cuts the requirement of two or more muons would keep the rate at about 2 events per second. Asking for three muons passing the cuts makes triggering comfortably possible at almost any imaginable luminosity at the SSC.

Although viable, the above mentioned cut on the transverse momentum carried through over all four leptons is fairly severe.[13] Thus it is important to be able to work with lower transverse momenta, *i.e.* around 10 GeV/c at the same time. Single inclusive lepton triggers, like those involving leptons from the $W^{\pm}$ and Z^0 bosons, paired with some other trigger condition from elsewhere in the detector (calorimeter, muon system) or even running on their own, will have to live with higher thresholds beyond 20 GeV/c. This dynamic range aspect translates into requirements on the transverse momentum *resolution* of the trigger as can be seen in correlation plots of the transverse momentum against the measured change in the azimuthal angle φ in the model intermediate tracking system (Fig.8). It is immediately obvious that without any subdivision in polar angle or pseudorapidity it is impossible to set reasonably well defined thresholds for the transverse momentum. By looking at the projections onto the transverse momentum axis for various cuts (upper limits) on the measured change in φ (Fig.9), I find the number of four subdivisions quite appropriate as there is not much left to improve the sharpness of the thresholds up to well beyond 20 GeV/c. To have no subdivision at all clearly gives unacceptable threshold shapes as shown in Fig.10. The actual quality of the thresholds will then be determined by the precision with which the measurement of the φ coordinate for the purpose of the trigger can be made.

4. Summary

For a simple three-station intermediate tracking system to be useful for triggering, it has to be able to trigger on charged particles at transverse momenta from around 10 GeV/c (and possibly below) to well beyond 20 GeV/c. This can be achieved with a subdivision into bins of width $\Delta\eta = 0.2$ in pseudorapidity and a design capable of measuring changes in the azimuthal angle of a track across the three stations down to $\Delta\varphi \approx 1$ $mrad$. These requirements seem to be within reach of the technologies currently being developed for tracking in the intermediate angle region.[4,5] Since the present work had been started about 10 months ago and evolved over time, other studies got under way, looking at more detailed designs of the tracking system and trigger setup,[14] reaching and using conclusions and requirements in agreement with those I have obtained in the present work.

ACKNOWLEDGEMENTS

I am very grateful for the interest, guidance and encouragement I have received from all members of the Intermediate Tracking Detector group in SDC, and to Dr. Torbjørn Sjøstrand for his advice on some problems I happened to encounter in using the PYTHIA program.

REFERENCES

1) EHIT Collaboration, J.M.Bailey *et al.*, Forward Tracking with Enhanced Electron Identification, Proceedings of the Symposium on Detector Research and Development for the Superconducting Super Collider, Fort Worth, Texas, October 15-18, 1990, eds. T.Dombeck, V.Kelly and G.P. Yost, World Scientific Publishing Co.Pte.Ltd., Singapore 1991, p.202, and SDC-90-00148

2) Solenoid Detector Collaboration, G.H.Trilling *et al.*, SDC-90-00085 and SSC-EOI-3, SSC Laboratory, Dallas, Texas, May 24, 1990, and SDC-90-00151 and SSC-LOI-1, SSC Laboratory, Dallas, Texas, November 30, 1990

3) E.Eichten, I.Hinchliffe, K.Lane and C.Quigg, Rev.Mod.Phys. 56 (1984) 579; erratum Rev.Mod.Phys. 58 (1986) 1065

4) E.F.Barasch *et al.*, The Microstrip Chamber - Ultraprecise Tracking for SSC Detectors, Proceedings of the Symposium on Detector Research and Development for the Superconducting Super Collider, Fort Worth, Texas, October 15-18, 1990, eds. T.Dombeck, V.Kelly and G.P.Yost, World Scientific Publishing Co.Pte.Ltd., Singapore 1991, p.209

5) A.Sill, Advanced Field Shaping Drift Chambers for SSC Forward Tracking, Proceedings of the Symposium on Detector Research and Development for the Superconducting Super Collider, Fort Worth, Texas, October 15-18, 1990, eds. T.Dombeck, V.Kelly and G.P.Yost, World Scientific Publishing Co.Pte.Ltd., Singapore 1991, p.655, and SDC-90-00143

6) Suggested to me by John Elias, Fermilab, private communication

7) H.U.Bengtsson and T.Sjøstrand, The Lund Monte Carloe for Hadronic Processes - PYTHIA version 5.4, University of Lund, Lund, Sweden and CERN, Geneva, Switzerland, June 1990 (unpublished); cf. also H.U.Bengtsson and T.Sjøstrand, The Lund Monte Carlo for Hadronic Processes - PYTHIA version 4.8, internal report LU TP 87-3, University of Lund, Lund, Sweden, and UCLA-87-001, University of California, Los Angleles, California, U.S.A., January 1987

8) T.Sjøstrand, private communication

9) R.N.Cahn *et al.*, Proceedings of the Workshop on Experiments, Detectors, and Experimental Areas for the Supercollider, July 7-17, 1987, Berkeley, California, eds. R.Donaldson and M.G.D.Gilchriese, World Scientific Publishing Co.Pte.Ltd., Singapore 1988, p.20

10) R.Thun *et al.*, Proceedings of the Workshop on Experiments, Detectors, and Experimental Areas for the Supercollider, July 7-17, 1987, Berkeley, California, eds. R.Donaldson and M.G.D.Gilchriese, World Scientific Publishing Co.Pte.Ltd., Singapore 1988, p.78

11) E.M.Wang *et al.*, Proceedings of the 1988 DPF Summer Study on High Energy Physics in the 1990's, Snowmass, Colorado, June 27 - July 15, 1988, ed. S.Jensen, World Scientific Publishing Co.Pte.Ltd., Singapore 1989, p.109

12) U.Nauenberg, A study of kinematic properties of the muons from Higgs decay, SDC-90-00091, November 1990

13) R.M.Barnett, K.Einsweiler and I.Hinchliffe, Higgs detection via decays to leptons with the SDC detector, SDC-90-00099, November 1990

14) See *e.g.* the presentations of Steve Maxfield, University of Liverpool, and Alan Sill, University of Rochester, at the SDC Collaboration Meeting at Oak Ridge, September 1991

TABLE CAPTIONS

1. Cross sections for selected processes with different minimum muon multiplicity requirements and without and with cuts.

FIGURE CAPTIONS

1. Bending power versus pseudorapidity a) as shown in Fig.9 of the SDC LoI,[2] b) as approximated for use in the present study. The approximation is no worse than 10% off for the iron loaded version and much better for the air core magnet version.

2. Distribution of inclusive muons over rapidity for some selected processes from one SSC year of luminosity, 10 fb^{-1}. Note that in the left half, the rates are given in units of 10^6 muons unlike in the right half which shows unscaled rates.

3. Distributions of inclusive muons over transverse momentum for some selected processes from one year of SSC luminosity. Note the different scales in the two parts, similar as in Fig.2.

4. Transverse momenta of inclusive muons in four bins of pseudorapidity on a linear (left) and logarithmic scale (right).

5. Multiplicity distributions of inclusive muons for selected processes without any cuts, normalized to one SSC year of luminosity. Note that the background processes are scaled down again.

6. Multiplicity distributions of inclusive muons passing the basic cuts $p_t \geq 20\ GeV/c$ and $|\eta| \leq 2.5$, normalized to one year of SSC luminosity.

7. Acceptance for at least two muons with $p_{t,\mu} \geq 20\ GeV/c$ (solid lines), at least three (dashed) and at least four (dotted). In the upper plots all such muons are used irrespective of their source, in the middle only those from decays $W \rightarrow \mu\nu_\mu$ and in the bottom plots only those from $Z^0 \rightarrow \mu^+\mu^-$ decays are used.

8. Correlation between transverse momentum and measured change in the azimuthal angle, $\Delta\varphi = |\varphi_3 - \varphi_1|$, for the four bins of pseudorapidity and the full range, $|\eta| = 1.7 - 2.5$, for different processes. The vertical band-like fine structure is an artefact of the histogramming software.

9. Efficiency over transverse momentum for different maximum measured changes in the azimuthal angle across the three station of the intermediate tracking system, $\Delta\varphi = |\varphi_3 - \varphi_1|$, for four bins in pseudorapidity. The air core version of the magnet has been assumed for getting the field integrals from Fig.1.

10. Efficiency over transverse momentum as in Fig.9 but for the range $|\eta| = 1.7 - 2.5$ in a single bin with the radii fixed at the center of the polar angle range.

Table 1: Cross sections (in nb)

a) Total cross section and cross sections for minimum required muon multiplicities

	σ_{tot}	$\sigma_{\geq 2\mu}$	$\sigma_{\geq 3\mu}$	$\sigma_{\geq 4\mu}$	1 *event*
QCD	$9.64 \cdot 10^7$	$2.37 \cdot 10^5$	$1.25 \cdot 10^4$	241.	241.
$b\bar{b}$	$2.60 \cdot 10^5$	$2.16 \cdot 10^4$	2140.	78.0	8.66
$t\bar{t}$	12.4	2.08	0.496	0.0860	$3.09 \cdot 10^{-4}$
Z^0	126.	13.9	0.521	0.047	$3.14 \cdot 10^{-3}$
$Z^0 + jet$	30.8	2.14	0.27	0.036	$7.70 \cdot 10^{-3}$
$Z^0 Z^0$	0.0257	$3.14 \cdot 10^{-3}$	$5.46 \cdot 10^{-4}$	$1.18 \cdot 10^{-4}$	$6.42 \cdot 10^{-7}$
$H(400)$	0.0517	$5.78 \cdot 10^{-3}$	$1.19 \cdot 10^{-3}$	$2.23 \cdot 10^{-4}$	$1.29 \cdot 10^{-6}$
$H(140)$	0.110	$9.63 \cdot 10^{-3}$	$1.42 \cdot 10^{-3}$	$21.4 \cdot 10^{-4}$	$2.74 \cdot 10^{-6}$
$Z^0 Z^0 \rightarrow 4\mu$	$3.77 \cdot 10^{-5}$	$3.77 \cdot 10^{-5}$	$3.77 \cdot 10^{-5}$	$3.77 \cdot 10^{-5}$	$3.77 \cdot 10^{-9}$
$H(400) \rightarrow 4\mu$	$1.55 \cdot 10^{-5}$	$1.55 \cdot 10^{-5}$	$1.55 \cdot 10^{-5}$	$1.55 \cdot 10^{-5}$	$1.55 \cdot 10^{-9}$
$H(140) \rightarrow 4\mu$	$6.65 \cdot 10^{-6}$	$6.65 \cdot 10^{-6}$	$6.65 \cdot 10^{-6}$	$6.65 \cdot 10^{-6}$	$6.65 \cdot 10^{-10}$

Note that the cross section in nb is equal to the event rate (in s^{-1}) at the SSC design luminosity. The event yield per nominal SSC year is thus obtained by multiplying the numbers as given in the table by 10^7. The statistical accuracy of the simulation is indicated by the cross section corresponding to one event in the rightmost column.

All cross sections are given for transverse momenta of the hard scattering process above $q_{t,min} = 1\ GeV/c$, except $Z^0 + jet$ at $q_{t,min} = 25\ GeV/c$. The cross section in this last case is somewhat overestimated (probably less than an order of magnitude) due to divergence of the cross section calculation at small q_t.[8]

Table 1: Cross sections (in nb)

b) Cross sections for minimum required muon multiplicities with cuts $p_t \geq 20\ GeV/c$ and $|\eta| \leq 2.5$

	$\sigma_{\geq 2\mu}{}^{cut}$	$\sigma_{\geq 3\mu}{}^{cut}$	$\sigma_{\geq 4\mu}{}^{cut}$	1 *event*
QCD	$(< 241.)$			241.
$b\bar{b}$	(< 8.66)			8.66
$t\bar{t}$	0.195	$9.99 \cdot 10^{-3}$	$3.09 \cdot 10^{-4}$	$3.09 \cdot 10^{-4}$
Z^0	1.03	$(< 3.14 \cdot 10^{-3})$		$3.14 \cdot 10^{-3}$
$Z^0 + jet$	0.444	$5.39 \cdot 10^{-3}$	$(< 7.70 \cdot 10^{-3})$	$7.70 \cdot 10^{-3}$
$Z^0 Z^0$	$8.57 \cdot 10^{-4}$	$2.25 \cdot 10^{-5}$	$3.21 \cdot 10^{-6}$	$6.42 \cdot 10^{-7}$
$H(400)$	$1.32 \cdot 10^{-3}$	$6.33 \cdot 10^{-5}$	$1.16 \cdot 10^{-5}$	$1.29 \cdot 10^{-6}$
$H(140)$	$5.07 \cdot 10^{-4}$	$1.37 \cdot 10^{-5}$	$2.74 \cdot 10^{-6}$	$2.74 \cdot 10^{-6}$
$Z^0 Z^0 \rightarrow 4\mu$	$2.66 \cdot 10^{-5}$	$1.81 \cdot 10^{-5}$	$8.62 \cdot 10^{-6}$	$3.77 \cdot 10^{-9}$
$H(400) \rightarrow 4\mu$	$1.30 \cdot 10^{-5}$	$1.11 \cdot 10^{-5}$	$8.68 \cdot 10^{-5}$	$1.55 \cdot 10^{-9}$
$H(140) \rightarrow 4\mu$	$4.90 \cdot 10^{-6}$	$3.06 \cdot 10^{-6}$	$6.13 \cdot 10^{-7}$	$6.65 \cdot 10^{-10}$

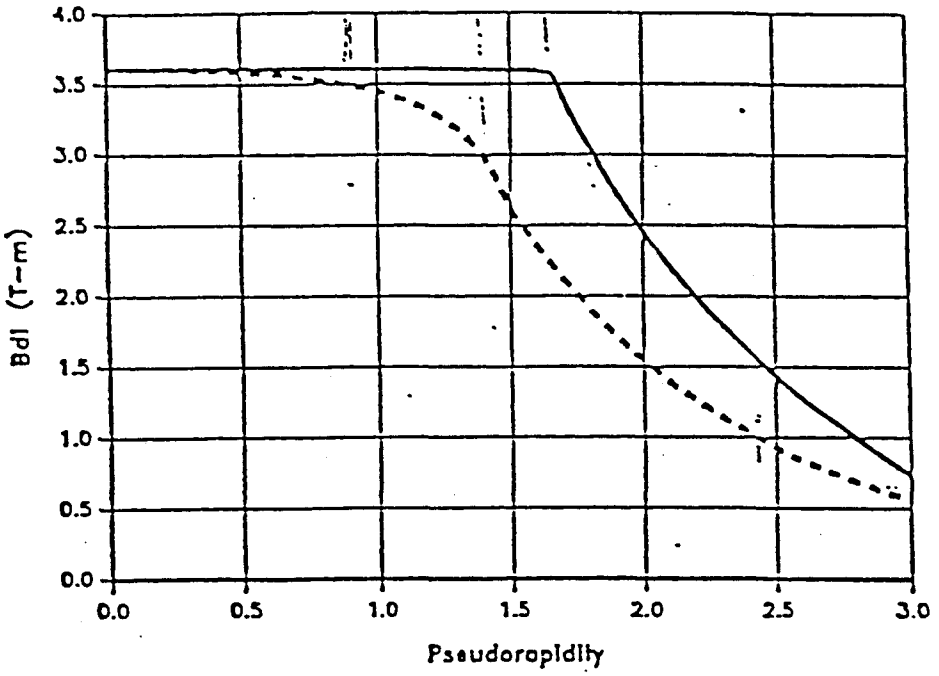

LoI-FIG. 9. Bending power versus pseudorapidity for a Type-U solenoid with (a) iron endcap calorimetry and (b) nonmagnetic endcap calorimetry.

Fig. 1a

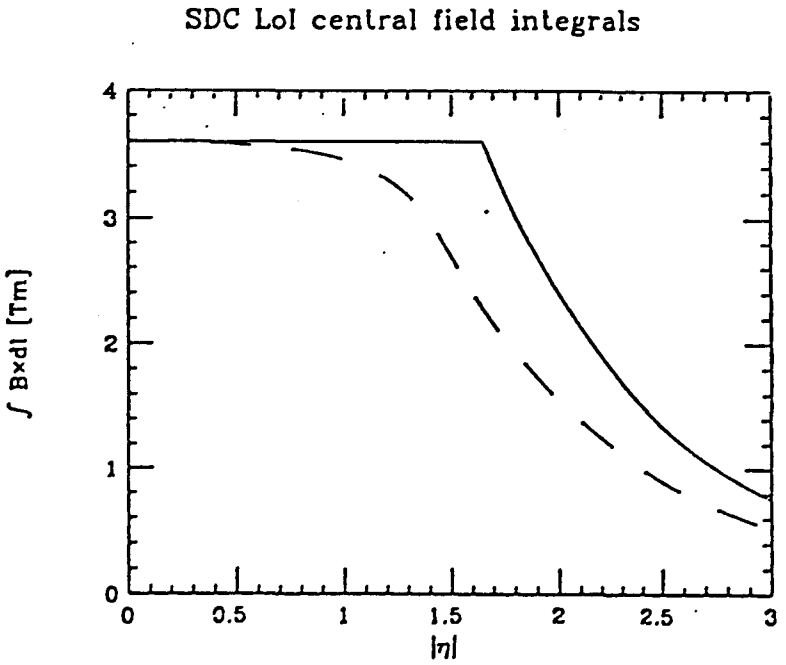

Fig. 1b

Rapidity distributions of inclusive muons

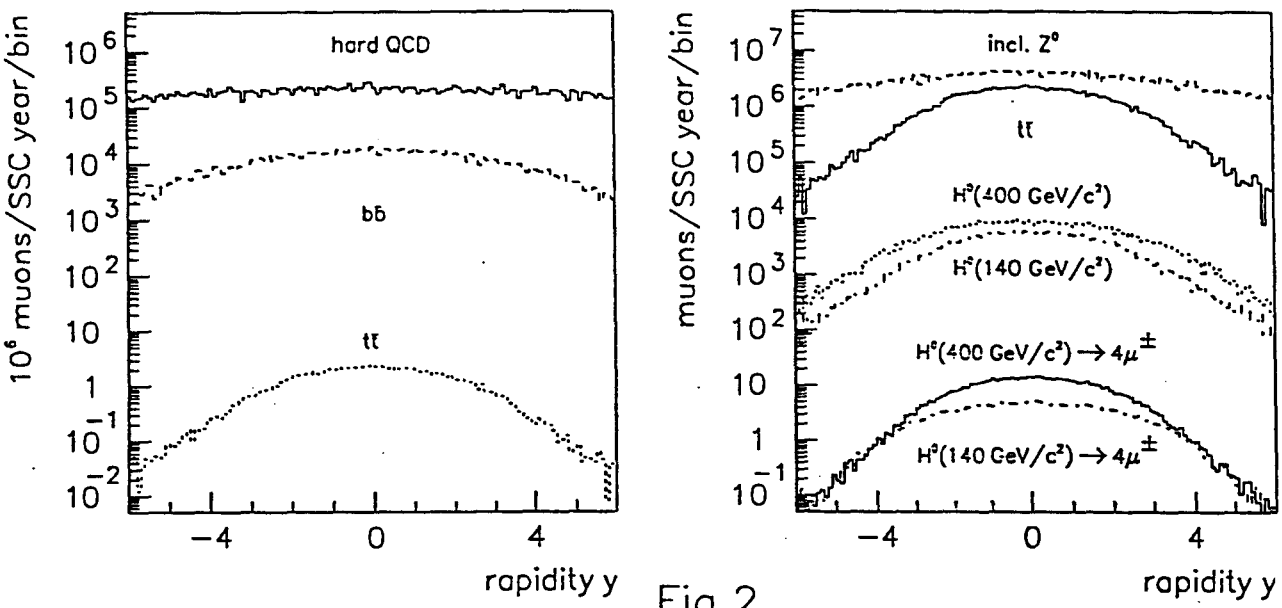

Fig.2

Transverse momentum distributions of inclusive muons

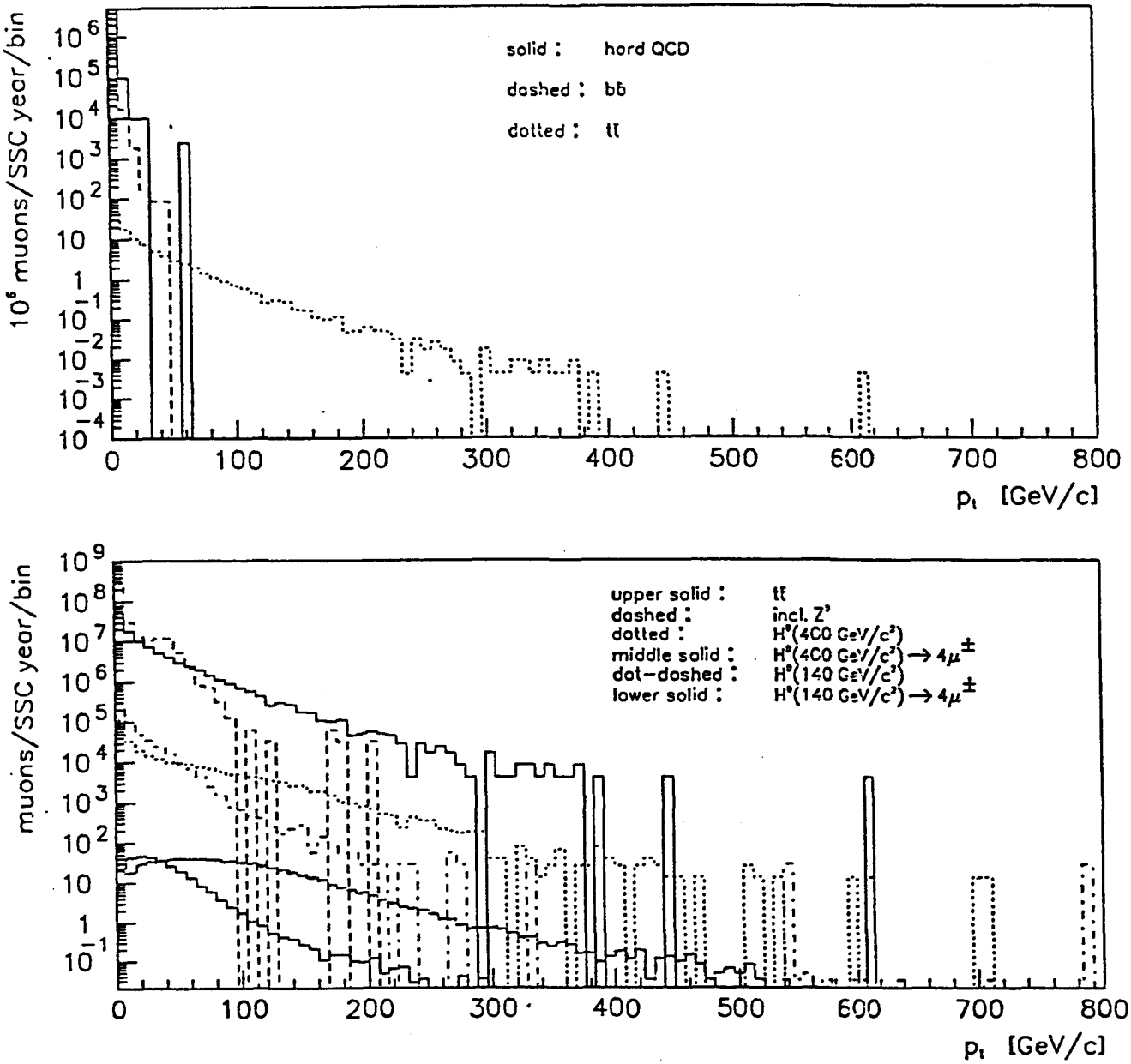

Fig.3

$p_t(\mu)$ in bins of $|\eta|$

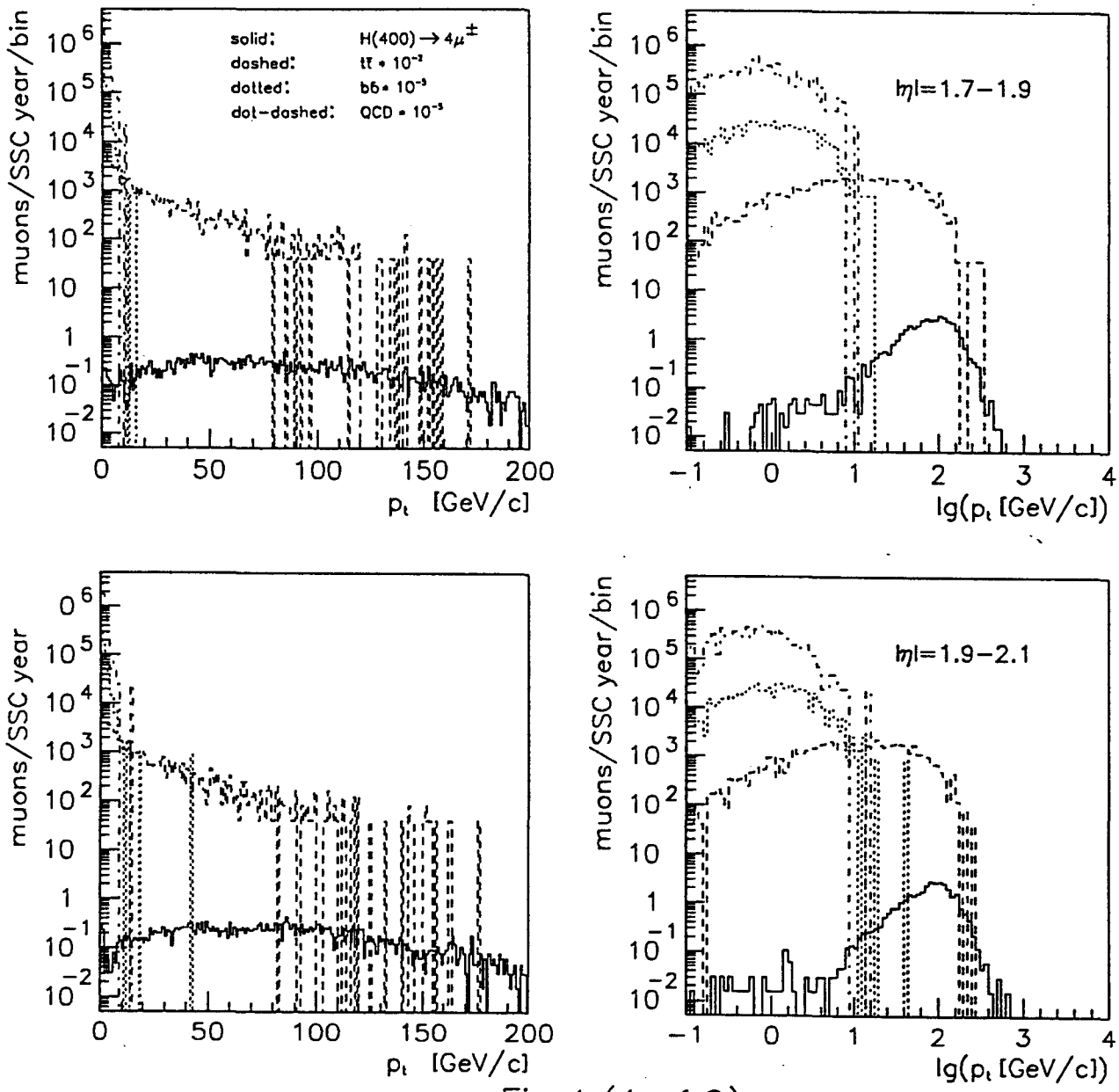

Fig.4 (1 of 2)

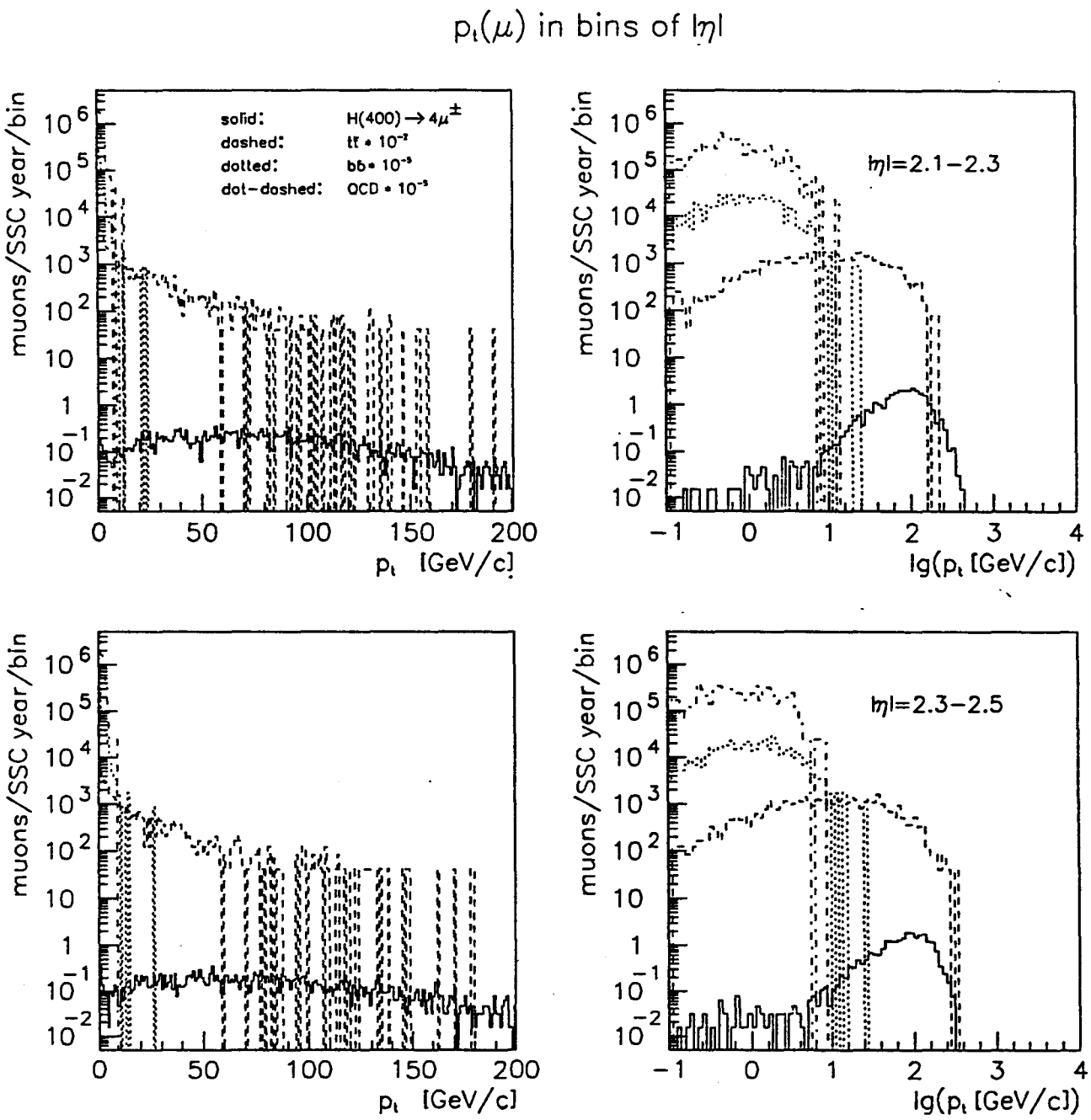
$p_t(\mu)$ in bins of $|\eta|$
solid: H(400) → 4μ±
dashed: tt̄ * 10⁻²
dotted: bb̄ * 10⁻⁵
dot-dashed: QCD * 10⁻⁵
muons/SSC year/bin
p_t [GeV/c]
$|\eta|$=2.1−2.3
$|\eta|$=2.3−2.5
lg(p_t [GeV/c])

Fig.4 (2 of 2)

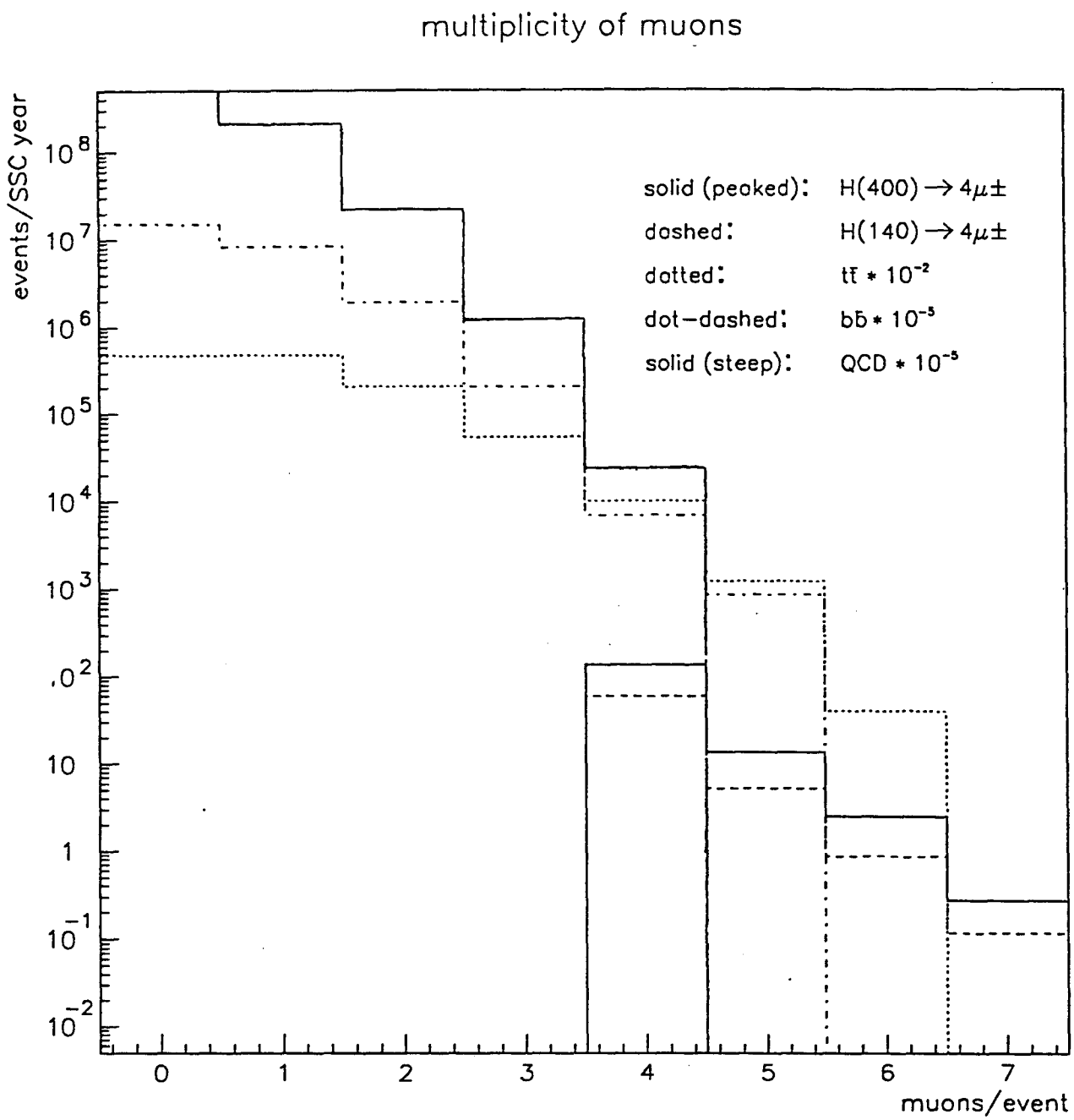
multiplicity of muons
events/SSC year
solid (peaked): H(400) → 4μ±
dashed: H(140) → 4μ±
dotted: tt̄ * 10⁻²
dot-dashed: bb̄ * 10⁻⁵
solid (steep): QCD * 10⁻⁵
muons/event

Fig.5

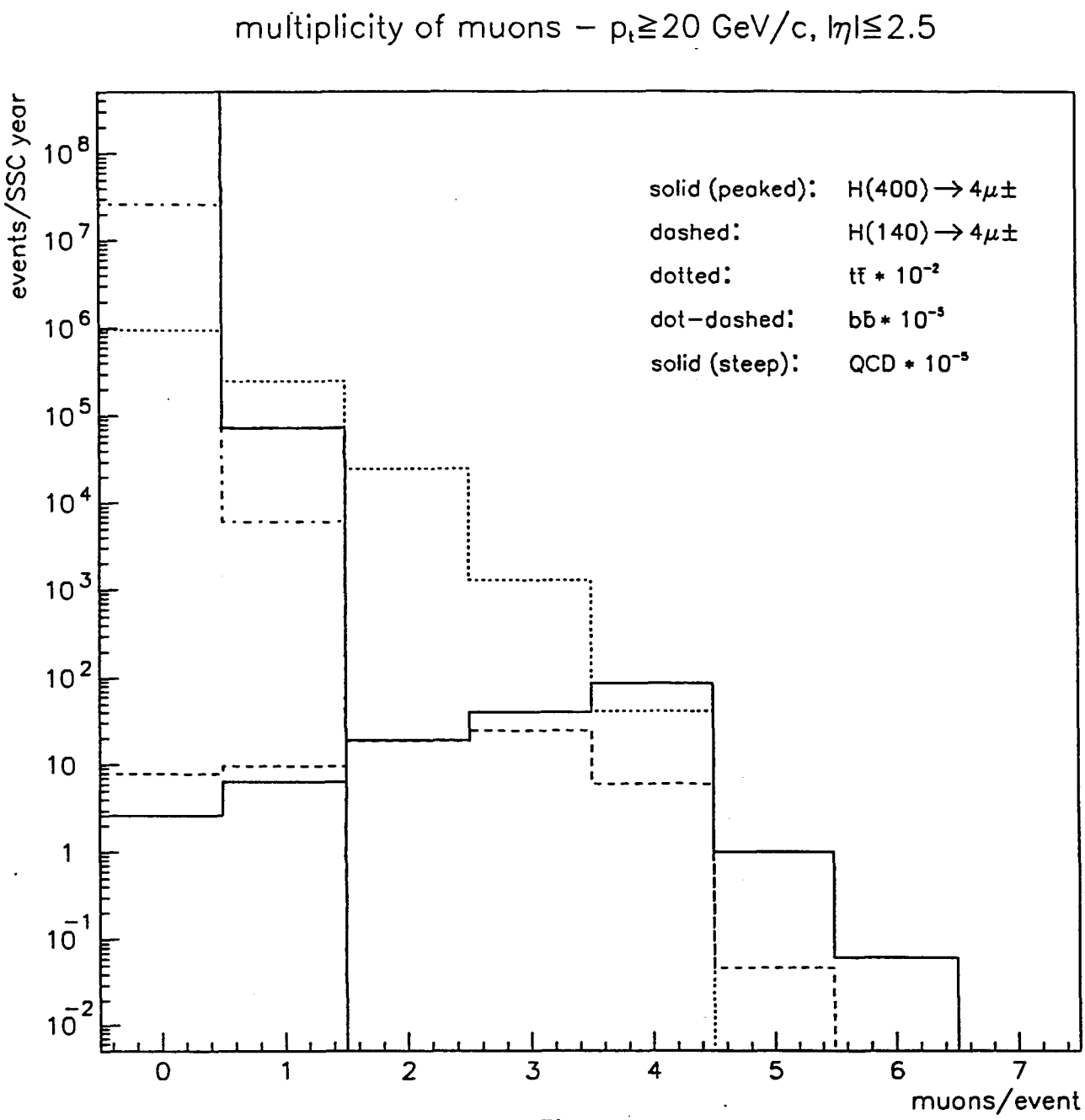
multiplicity of muons – $p_t \geq 20$ GeV/c, $|\eta| \leq 2.5$
events/SSC year
10^8
10^7
10^6
10^5
10^4
10^3
10^2
10
1
10^{-1}
10^{-2}
solid (peaked): H(400) → 4μ±
dashed: H(140) → 4μ±
dotted: $t\bar{t} * 10^{-2}$
dot–dashed: $b\bar{b} * 10^{-5}$
solid (steep): QCD * 10^{-5}
0
1
2
3
4
5
6
7
muons/event

Fig.6

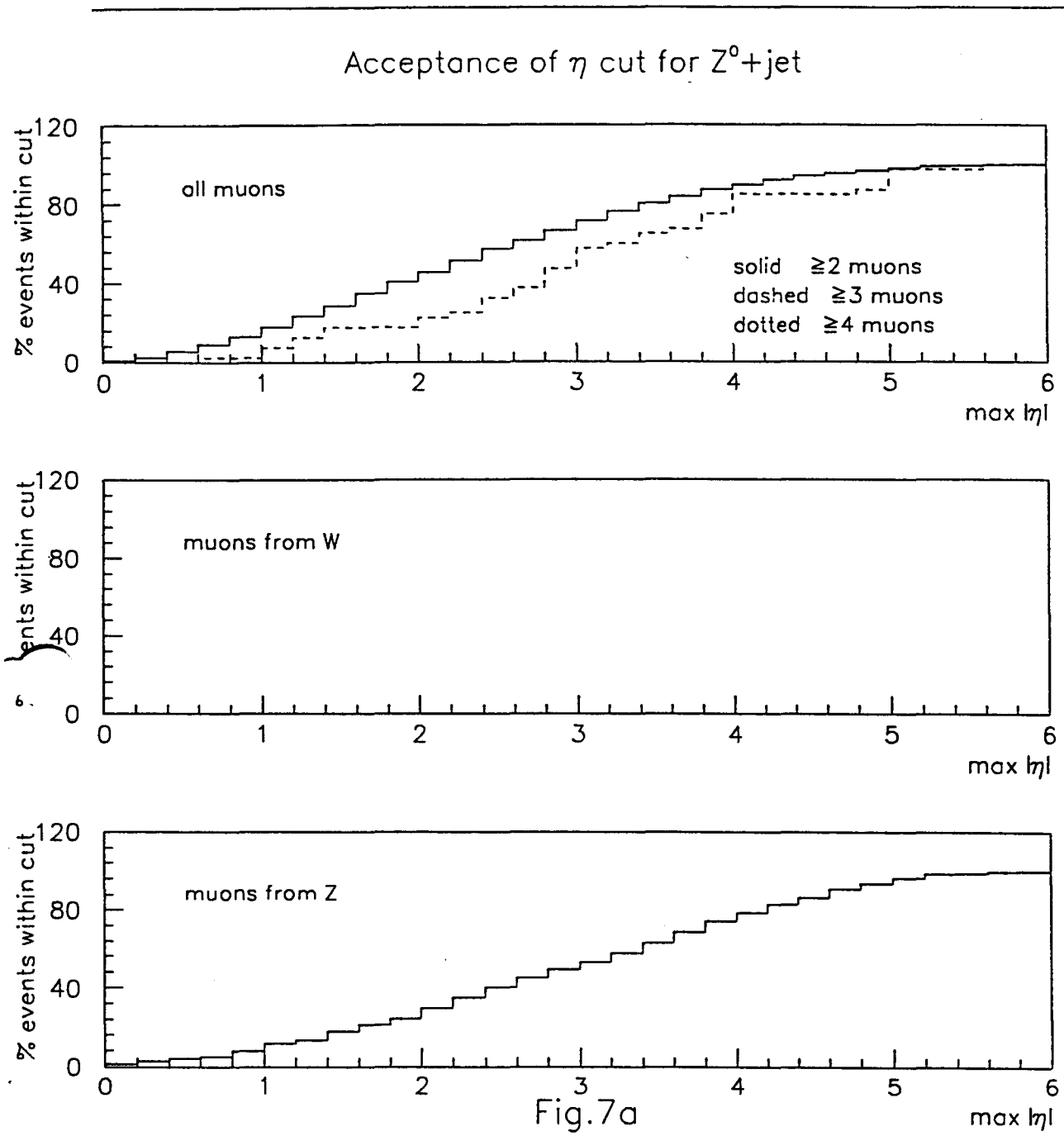
Acceptance of η cut for Z°+jet
% events within cut
all muons
solid ≧2 muons
dashed ≧3 muons
dotted ≧4 muons
max |η|
muons from W
muons from Z
0
40
80
120
1
2
3
4
5
6

Fig.7a

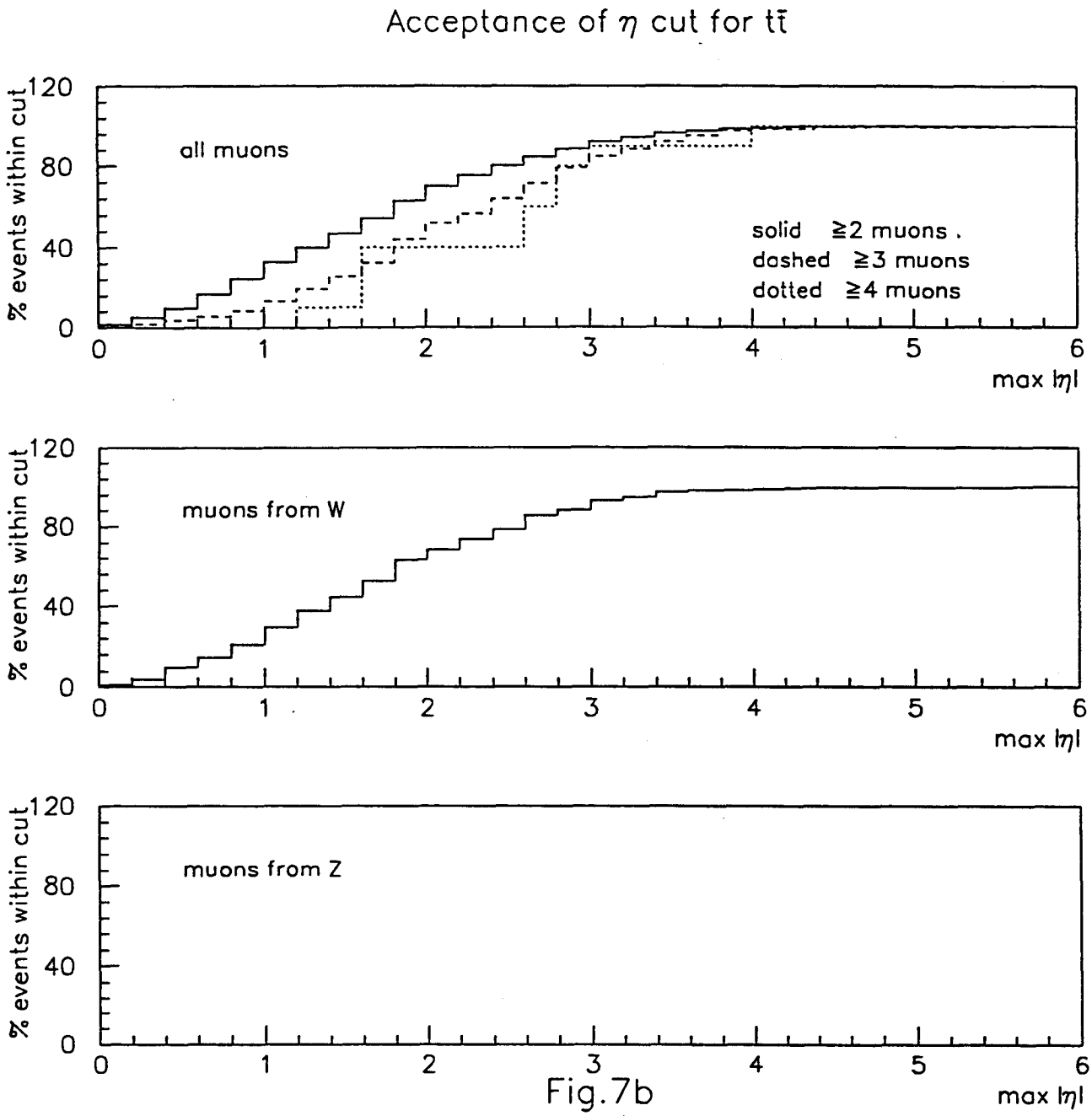
Acceptance of η cut for tt̄
% events within cut
all muons
solid ≧2 muons
dashed ≧3 muons
dotted ≧4 muons
max |η|
muons from W
muons from Z
0
40
80
120
0
1
2
3
4
5
6

Fig.7b

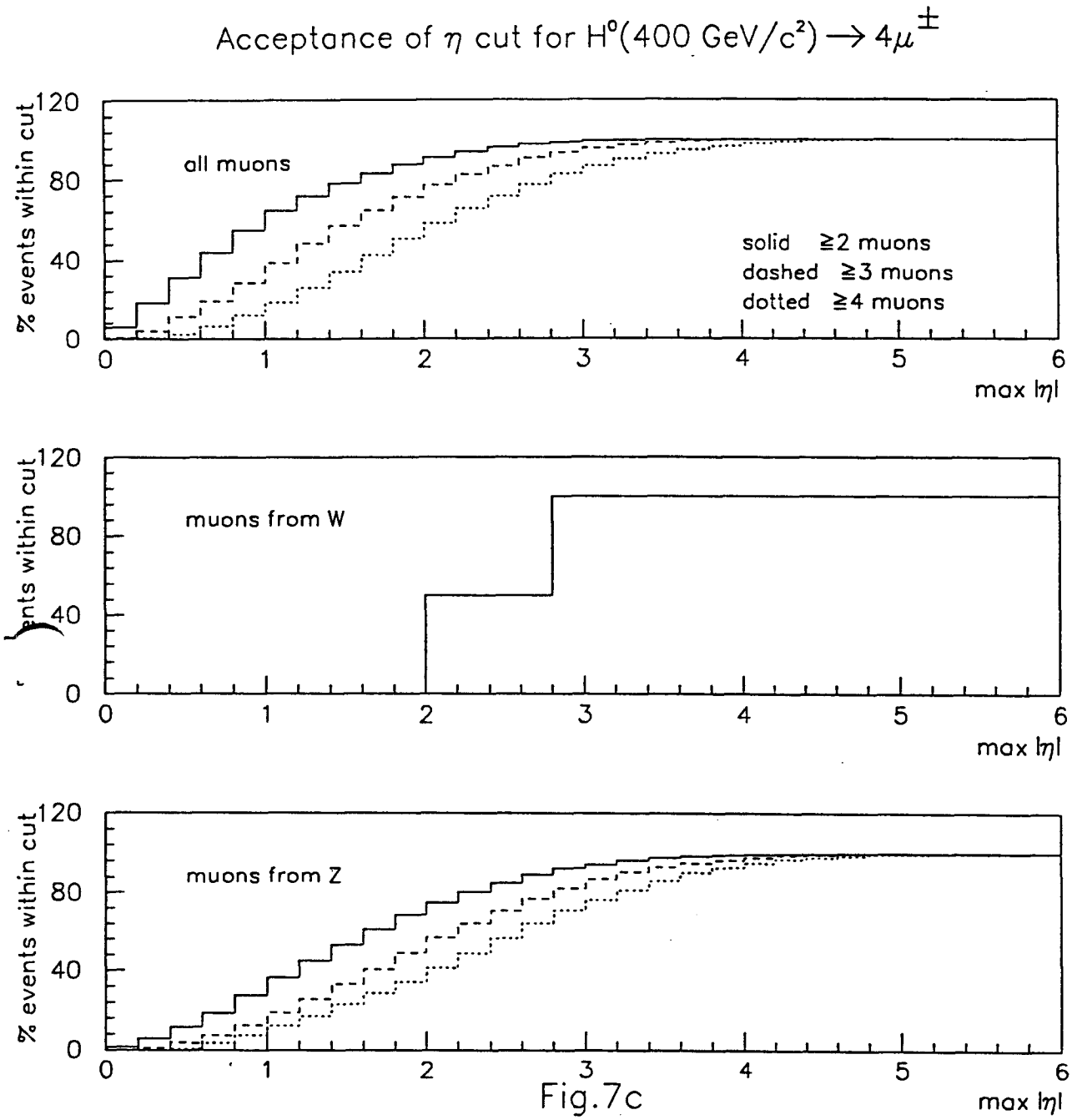
Acceptance of η cut for H°(400 GeV/c²) → 4μ±
% events within cut
all muons
solid ≧2 muons
dashed ≧3 muons
dotted ≧4 muons
max |η|
muons from W
muons from Z
0
40
80
120
1
2
3
4
5
6

Fig.7c

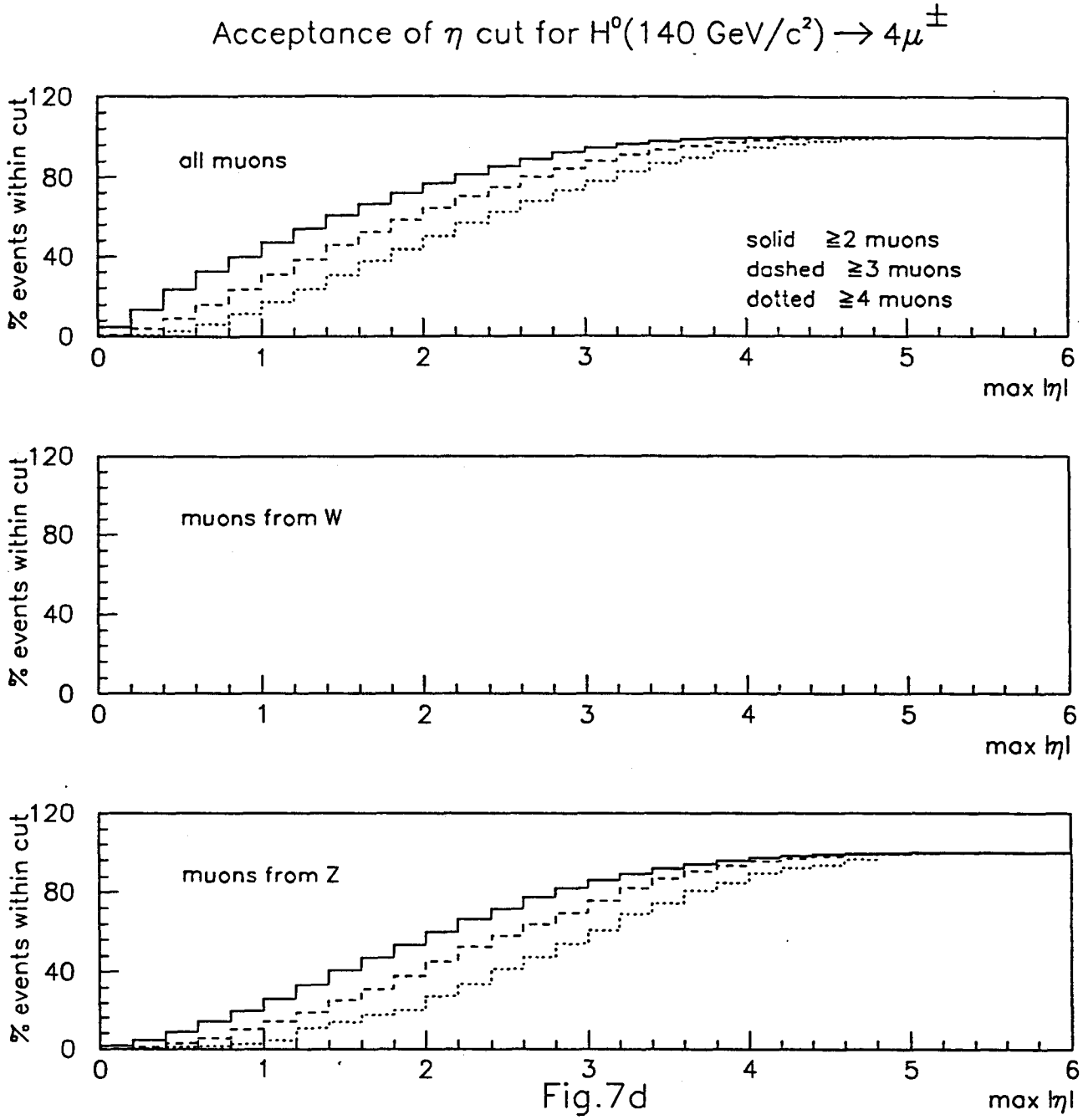
Acceptance of η cut for H°(140 GeV/c²) → 4μ±
% events within cut
all muons
solid ≧2 muons
dashed ≧3 muons
dotted ≧4 muons
max |η|
muons from W
muons from Z
0
40
80
120
1
2
3
4
5
6

Fig.7d

p_t versus measured $\Delta\varphi$ – $b\bar{b}$

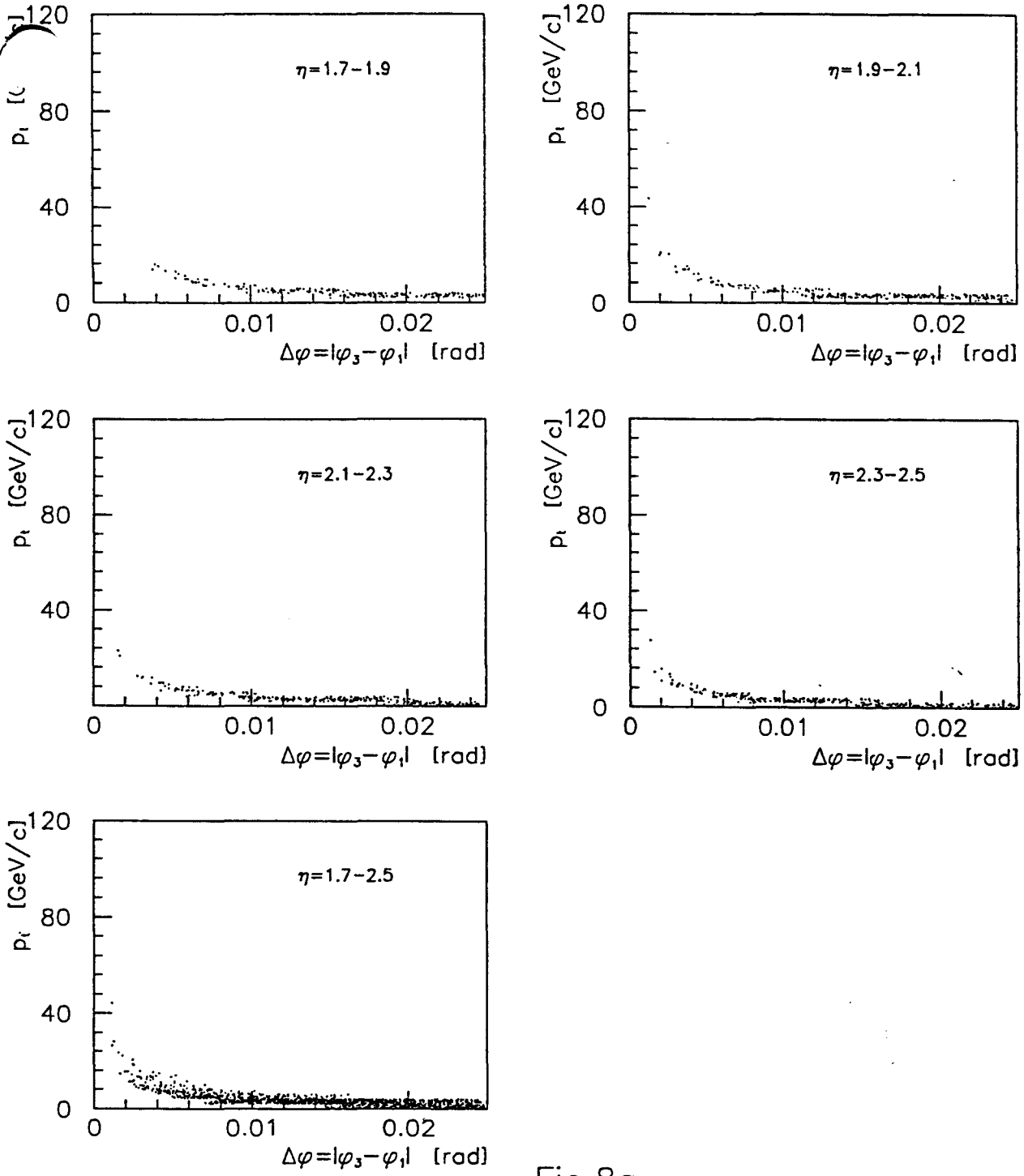

Fig.8a

p_t versus measured $\Delta\varphi - t\bar{t}$

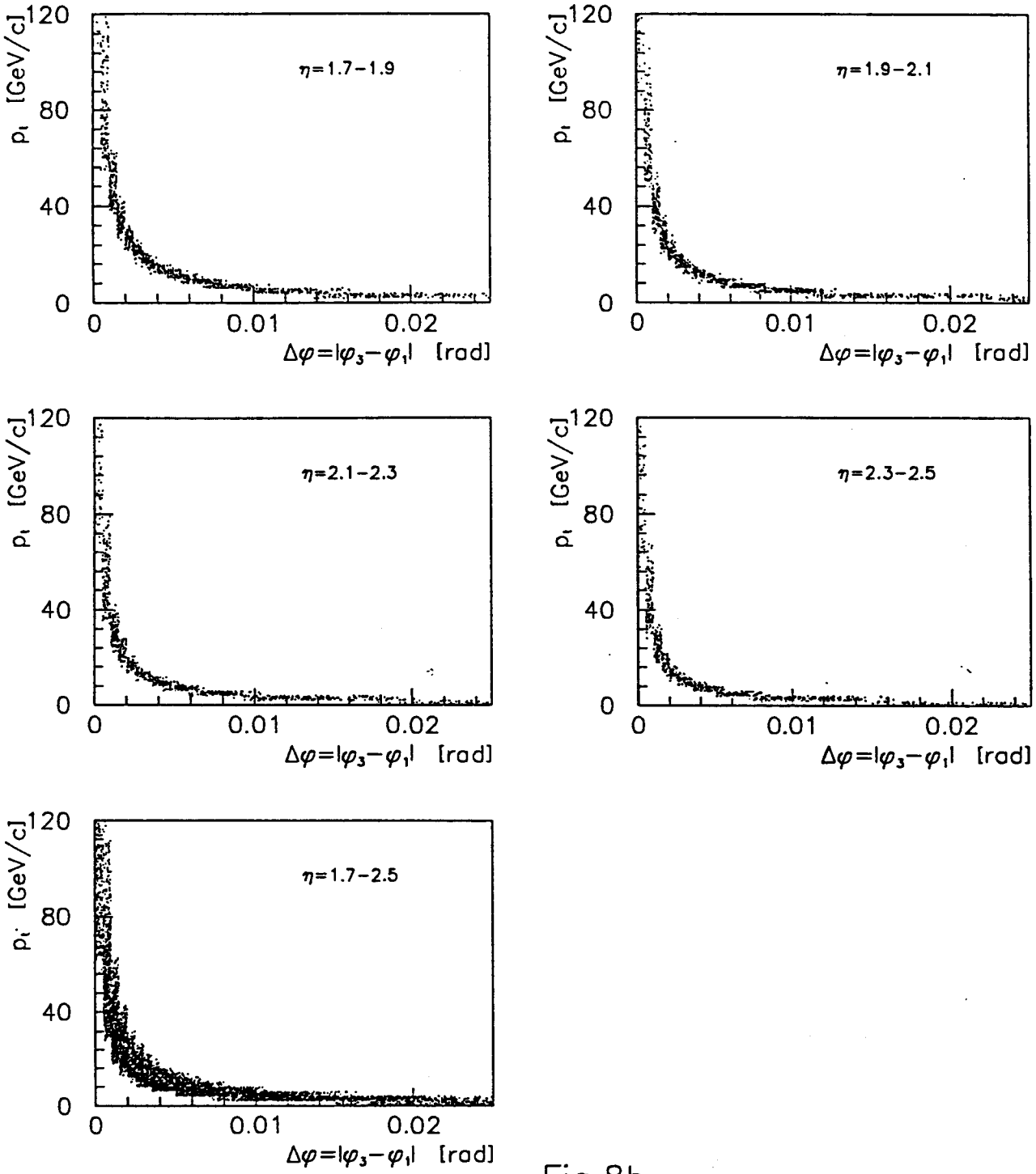

Fig.8b

p_t vs. measured $\Delta\varphi$ – $H^0(400\ GeV/c^2) \rightarrow 4\mu^{\pm}$

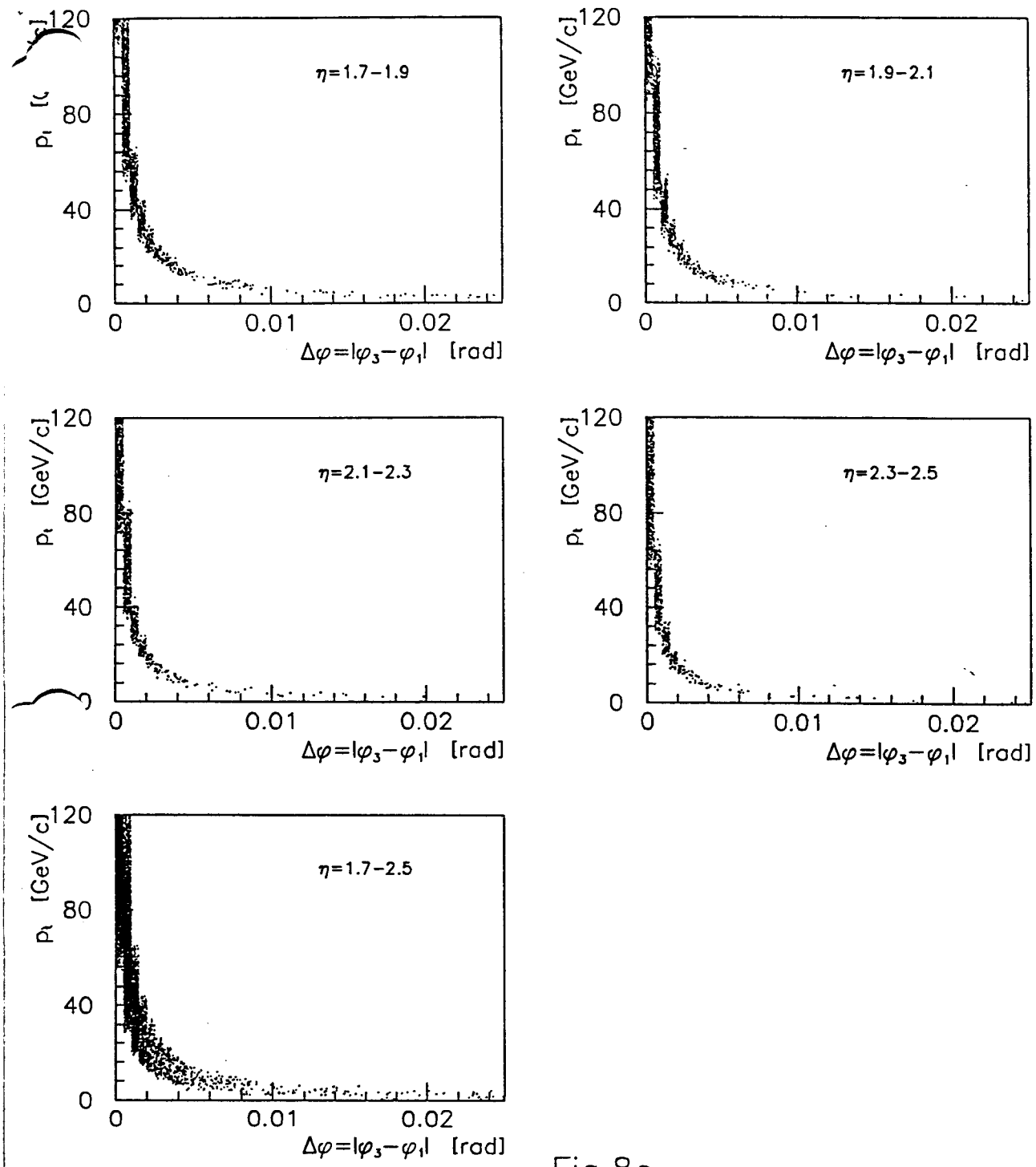

Fig.8c

p_t vs. measured $\Delta\varphi$ – $H^0(140\ GeV/c^2) \rightarrow 4\mu^{\pm}$

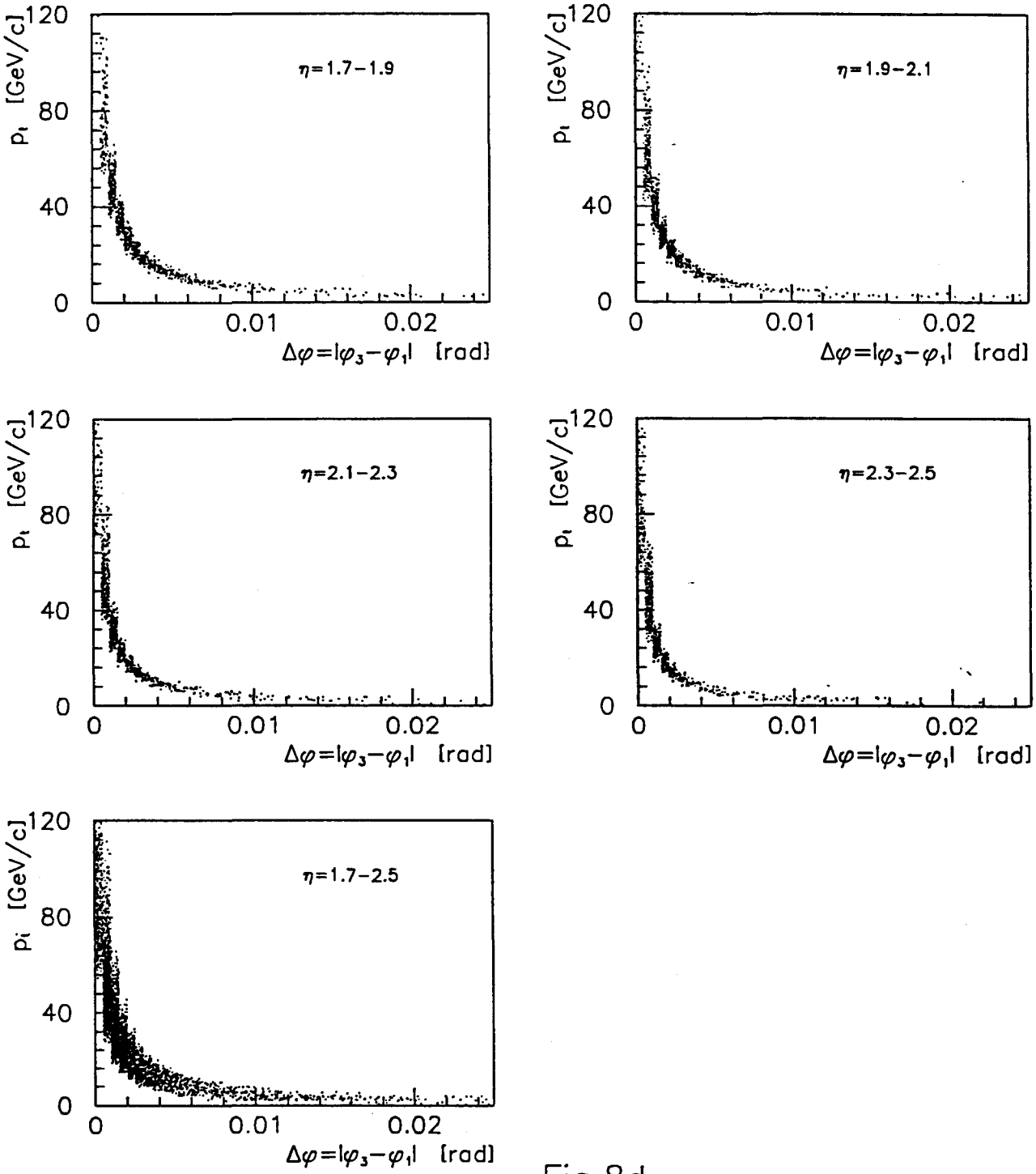

Fig.8d

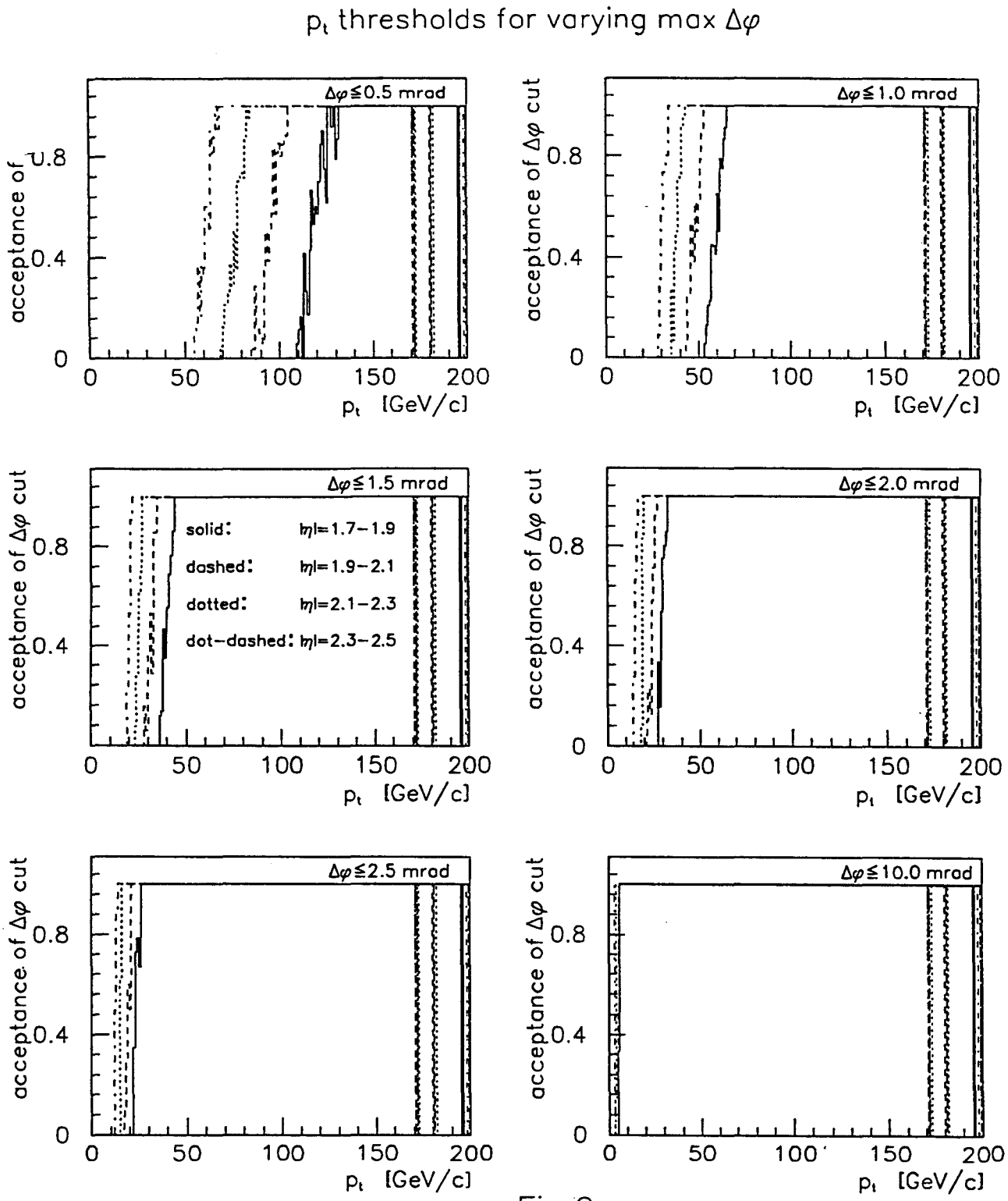
p_t thresholds for varying max $\Delta\varphi$
$\Delta\varphi \leq 0.5$ mrad
$\Delta\varphi \leq 1.0$ mrad
$\Delta\varphi \leq 1.5$ mrad
$\Delta\varphi \leq 2.0$ mrad
$\Delta\varphi \leq 2.5$ mrad
$\Delta\varphi \leq 10.0$ mrad
solid: $|\eta|=1.7-1.9$
dashed: $|\eta|=1.9-2.1$
dotted: $|\eta|=2.1-2.3$
dot-dashed: $|\eta|=2.3-2.5$
acceptance of $\Delta\varphi$ cut
p_t [GeV/c]

Fig.9

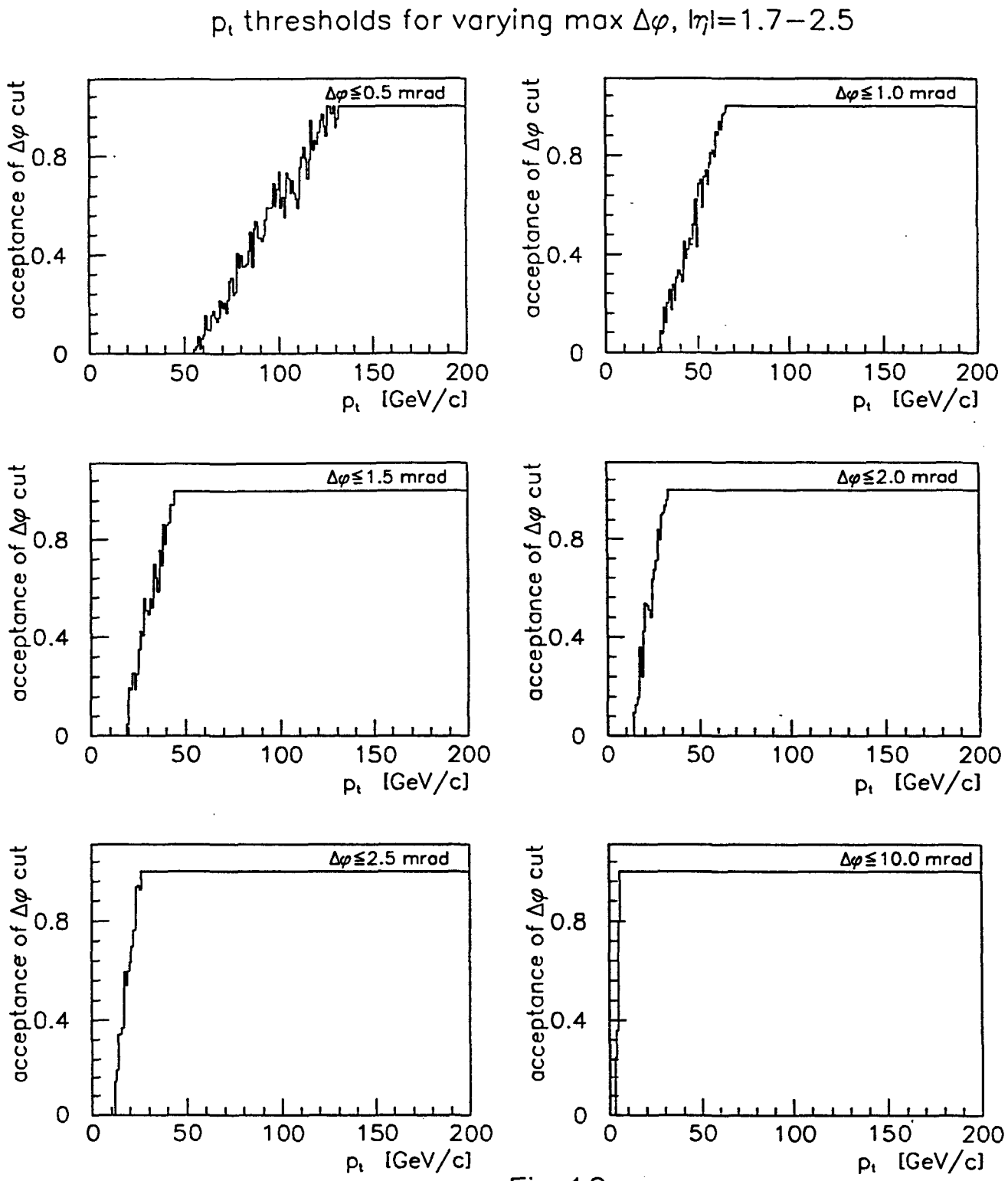
p_t thresholds for varying max $\Delta\varphi$, $|\eta|=1.7-2.5$
$\Delta\varphi \leq 0.5$ mrad
$\Delta\varphi \leq 1.0$ mrad
$\Delta\varphi \leq 1.5$ mrad
$\Delta\varphi \leq 2.0$ mrad
$\Delta\varphi \leq 2.5$ mrad
$\Delta\varphi \leq 10.0$ mrad
acceptance of $\Delta\varphi$ cut
p_t [GeV/c]
0
0.4
0.8
0
50
100
150
200

Fig.10